2082–2093 *Nucleic Acids Research, 2008, Vol. 36, No. 6* *Published online 14 February 2008*
doi:10.1093/nar/gkn054

The effect of sequence context on spontaneous Polζ-dependent mutagenesis in *Saccharomyces cerevisiae*

Amy L. Abdulovic[1,2], Brenda K. Minesinger[2] and Sue Jinks-Robertson[1,2,3,*]

[1]Department of Molecular Genetics and Microbiology, Duke University Medical Center, Durham, NC 27710, [2]Graduate Program in Biochemistry, Cell and Developmental Biology and [3]Department of Biology, Emory University, Atlanta, GA 30322, USA

Received October 2, 2007; Revised January 23, 2008; Accepted January 24, 2008

ABSTRACT

The Polζ translesion synthesis (TLS) DNA polymerase is responsible for over 50% of spontaneous mutagenesis and virtually all damage-induced mutagenesis in yeast. We previously demonstrated that reversion of the *lys2ΔA746* −1 frameshift allele detects a novel type of +1 frameshift that is accompanied by one or more base substitutions and depends completely on the activity of Polζ. These 'complex' frameshifts accumulate at two discrete hotspots (HS1 and HS2) in the absence of nucleotide excision repair, and accumulate at a third location (HS3) in the additional absence of the translesion polymerase Polη. The current study investigates the sequence requirements for accumulation of Polζ-dependent complex frameshifts at these hotspots. We observed that transposing 13 bp of identity from HS1 or HS3 to a new location within *LYS2* was sufficient to recapitulate these hotspots. In addition, altering the sequence immediately upstream of HS2 had no effect on the activity of the hotspot. These data support a model in which misincorporation opposite a lesion precedes and facilitates the selected slippage event. Finally, analysis of nonsense mutation revertants indicates that Polζ can simultaneously introduce multiple base substitutions in the absence of an accompanying frameshift event.

INTRODUCTION

DNA can acquire damage throughout the cell cycle and if the damage is not removed before being encountered during DNA synthesis, it can pose problems for the DNA replication machinery. The high-fidelity polymerases that replicate the bulk of genomic DNA possess geometrically constrained polymerase active sites, which render them intolerant to template base distortions (1). Thus, when a replicative polymerase encounters a physically distorted or noncoding lesion, it is likely to stall and processive replication at this site will cease. In response, the cell can employ two tolerance mechanisms to bypass the lesion: damage avoidance and translesion synthesis (TLS) (2). In damage avoidance, the newly replicated sister strand can be used as a template for DNA synthesis past the lesion. This can occur either through a strand-invasion process (homologous recombination) or through a strand-switching mechanism, which may involve fork regression. In TLS, the cell utilizes one or more low-fidelity polymerase(s) to insert a nucleotide across from the blocking lesion and/or extend from a lesion:base mispair (3). Relative to normal DNA synthesis, TLS is inherently error-prone; not only is there the potential of inserting an incorrect nucleotide across from a DNA lesion, but all TLS polymerases have low fidelity on undamaged DNA templates (4).

The yeast *Saccharomyces cerevisiae* contains three TLS polymerases: Polζ, Rev1 and Polη. Polζ, a member of the B family of DNA polymerases, is composed of two subunits: a catalytic subunit encoded by *REV3* and an

*To whom correspondence should be addressed. Tel: +919 681 7273; Fax: +919 684 2790; Email: sue.robertson@duke.edu
Present addresses:
Amy L. Abdulovic, Laboratory of Molecular Genetics, National Institute of Environmental Health Sciences, NIH, DHHS, Research Triangle Park, NC 27709, USA
Brenda K. Minesinger, Department of Biology, Massachusetts Institute of Technology, Cambridge, MA 02139, USA

The authors wish it to be known that, in their opinion, the first two authors should be regarded as joint First Authors

accessory protein encoded by *REV7* (5). TLS by Polζ can be error-prone or error-free depending on the lesion encountered. *In vitro*, for example, Polζ bypasses thymine glycols in an error-free manner (6) but bypasses thymine dimers in an error-prone manner (5). Although Polζ has the ability to insert a nucleotide across from many structurally deformed DNA bases *in vitro*, it has been speculated that the primary role for Polζ derives from its ability to extend from a primer:template mispair (7), an activity that is not exhibited by the replicative DNA polymerases. Polζ activity is highly mutagenic in yeast, with 50–75% of spontaneous mutagenesis and nearly 90% of induced mutagenesis being attributed to its activity (8,9).

Rev1 is a member of the Y family of TLS polymerases and exhibits deoxycytidyl transferase activity *in vitro*, incorporating a C across from lesions (10–12). Based on physical and genetic interactions with Polζ in yeast and mammalian cells (9,13–15), Rev1 has been hypothesized to facilitate Polζ-dependent TLS. Although Rev1 is required for most, if not all, Polζ-dependent mutagenesis in yeast, its catalytic activity does not always appear to be required for this process (Wiley,S. and Jinks-Robertson,S., unpublished data; (11,16). Polη (encoded by *RAD30*) is the third TLS polymerase in *S. cerevisiae* and, like Rev1, is a member of the Y family of DNA polymerases. *In vitro* TLS by Polη can be error-free, as in the bypass of a *cis-syn* thymine dimer or a 7,8-dihydro-8-oxoguanine (17,18), or error-prone, as in the bypass of a benzo[a]pyrine adduct (19). *In vivo*, loss of Polη has been observed to either increase or decrease mutagenesis in an assay-specific manner (20,21).

We previously described a chromosome-based assay that can monitor *in vivo* changes in Polζ-dependent mutagenesis occurring within the 150-bp 'reversion window' of the *lys2ΔA746* allele (22–25). In a nucleotide excision repair (NER)-defective background, compensatory +1 frameshifts that revert the *lys2ΔA746* allele are comprised of both simple and complex frameshifts. Simple frameshifts, defined as the insertion of a single nucleotide, account for more than half of the reversion events and are thought to occur primarily via DNA polymerase slippage in homopolymer runs. Complex frameshifts, defined as the insertion of a nucleotide accompanied by at least one base substitution within 6 nt of the selected frameshift event, account for ~30% of the reversion events and are absolutely dependent on the presence of Polζ (25).

The majority of the Polζ-dependent complex frameshift events in an NER-defective strain occur at two distinct hotspots within the reversion window, termed HS1 and HS2 (Figure 1; 25). The coding-strand sequences at these locations are similar: 5′-G*TTT*G**G** for HS1 and 5′-C*TTT***G**C for HS2. The complex events that accumulate at these hotspots are also similar, with the insertion of a T in the 3T run (in italics) usually being accompanied by a G → T transversion (G in bold) 3′ of the run. Because mutating the relevant G completely eliminates all frameshift events at HS1 and HS2, we have proposed that the initiating event for the complex frameshifts is a lesion at the corresponding G•C base pair (25). In addition, complex frameshift events at HS1 and HS2 are eliminated when cells are grown anaerobically, suggesting that the initiating lesion is oxidative in nature (22). These observations support a 'misincorporation-slippage' model, in which mutagenic bypass of a damaged base precedes and facilitates a subsequent slippage event. Given the direction of replication through the *LYS2* gene and the model that the relevant lesion is encountered 'before' the 3N run during DNA synthesis, the initiating damage would be to the guanine of the G•C base pair. While this model can account for the coupling between the predominant base substitution and the selected frameshift, ~50% of complex events contain another base substitution on the other side of the frameshift (25). We have suggested that these additional base substitutions reflect the extreme mutagenic potential of Polζ *in vivo*, and recent *in vitro* studies with purified proteins support this notion (26).

In addition to HS1 and HS2, a third hotspot for the accumulation of Polζ-dependent complex events (HS3, 5′-**C***AAA*T) becomes apparent when Polη is additionally deleted in an NER-defective background (Figure 1B; 23). The appearance of a third hotspot suggests a hierarchy in Polη versus Polζ usage, with the underlying lesion at HS3 being normally bypassed by Polη in a manner that is not detected in the *lys2ΔA746* system. Only in the absence of Polη does Polζ perform lesion bypass to produce its complex mutation signature at HS3. Strikingly, the pattern of complex frameshifts at HS3 is the reverse complement of that at HS2: an insertion of an A in the 3A run (in italics) most often associated with a C → A transversion at the 5′ C (in bold). Although this pattern is suggestive of a strand-specific bias for Polη, additional data suggest that the pattern more probably reflects a lesion-specific bias (23).

The complex signature of Polζ-dependent reversion events at HS1–HS3 provides a unique opportunity to investigate the sequence requirements at these positions. In the studies reported here, we demonstrate that hotspots can be functionally transposed to new locations within the *lys2ΔA746* reversion window, that the identity of sequence immediately upstream of HS2 is not important for hotspot activity, and that the occurrence of multiple Polζ-dependent base substitutions is not uniquely associated with frameshift mutagenesis. These results provide further insight into Polζ-dependent mutagenesis *in vivo*.

MATERIAL AND METHODS

Media and growth conditions

Cells were grown nonselectively in YEP medium (1% yeast extract, 2% Bacto-peptone, 250 mg/l adenine; 2% agar for plates) supplemented with either 2% dextrose (YEPD) or 2% glycerol + 2% ethanol (YEPGE). Selective growth was on synthetic complete medium supplemented with 2% dextrose (SCD) and lacking the appropriate nutrient (27). Selection of Ura^- segregants was on SCD–uracil medium supplemented with 12 μg/ml uracil and 1 mg/ml 5-fluoroorotic acid (5-FOA; 28). Lys^- segregants were selected on minimal medium

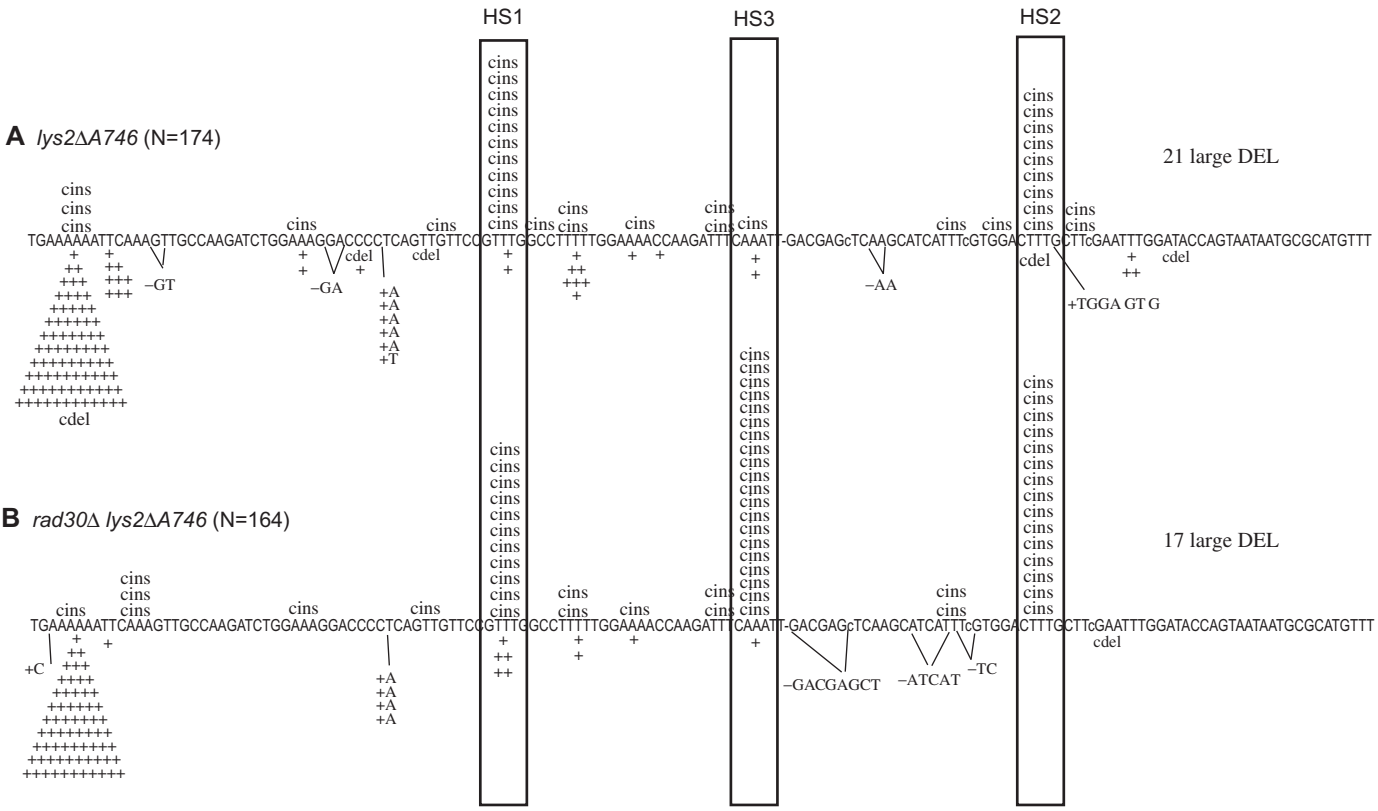

Figure 1. Reversion spectra of the *lys2ΔA746* allele in presence (*RAD30*) and absence (*rad30Δ*) of Polη. Spectra were generated in an NER-defective (*rad14Δ*) background and the number of revertants sequenced (*N*) is indicated next to the strain genotype. The nt deleted to create the *lys2ΔA746* allele is indicated by '—', and base substitutions introduced to extend the reversion window are indicated by lowercase letters (30). Insertions of a single nt are shown as '+' and complex insertions ('cins') are indicated above the sequence; complex deletions ('cdel') are shown below the sequence. Deletions of 95 bp or 131 bp with endpoints in short direct repeats are indicated as 'large DEL' and are above each spectrum. The boxed regions represent HS1, HS2 and HS3.

supplemented with 2 mg/ml α-aminoadipate (α-AA; 29). Geneticin-resistant or hygromycin-resistant transformants were selected on YEPD plates containing 200 μg/ml G418 or 300 μg/ml hygromycin B, respectively. All growth was at 30°C.

Plasmid construction

pSR786, a *URA3*-marked plasmid for introducing the *lys2ΔA746* allele, was constructed by subcloning a 1.2-kb XhoI/XbaI fragment from pSR585 (30) into XhoI/XbaI-digested pRS306 (31). pSR582 was constructed by first inserting a 1.2-kb XbaI/NaeI fragment containing the 5′ end of *LYS2* (from pDP6; 32) into XbaI/EcoRV-digested pRS303 (*HIS3*-containing integrating vector; 31). The resulting plasmid (pSR531) was then subjected to site-directed mutagenesis to introduce mutations A767C (removes a stop codon in an alternative reading frame; nt numbering is from the upstream XbaI site) and T781C (creates a BstBI site).

Plasmids containing a duplication of HS1 or HS3 were created as follows. First, complementary 18-nt oligonucleotides (oligos) were designed that contained 14 nt of homology to the hotspot to be duplicated, 4-nt complementary to BglII-generated overhangs at one end and nt changes necessary to remove stop codons in the duplicated sequence. The resulting oligos had 13 nt of identity to HS1 or HS3. The oligos hs1′F (5′-*gatc*CCG**TTTGG**CCTTTc) and hs1′R (5′-*gatc*gAAAGG**CCAAA**CGG) were used to duplicate HS1 (creates a TaqI site); oligos hs3′F (5′-*gatc*GATTT**CAAA**TTGcC) and hs3′R (5′*gatc*GgCAA**TTTG**AAATC) were used to duplicate HS3 (creates a ClaI site). BglII-compatible ends are in lowercase italics; duplicated sequences are in uppercase, with the core hotspot in bold; and sequence changes are in underlined lowercase. The appropriate oligo pairs (1 pmol of each) were incubated together at 65° for 5 min and then placed on ice. The annealed hs1′F/hs1′R mixture was ligated with 0.1 pmol of BglII-digested pSR786 to create pSR812 (*lys2ΔA746,hs1′*) and pSR813 (*lys2ΔA746,hs1′INV*), and the hs3′F/hs3′R mixture was ligated with 0.1 pmol of BglII-digested pSR817 (described below) to create pSR818 (*lys2ΔA746,hs3′,hs3mut*). Candidate clones were verified by sequencing.

Site-directed mutagenesis was performed on appropriate plasmids using the QuickChange kit (Stratagene) to create integrating plasmids with HS1 or HS3 mutated, with the 6A run disrupted, or with 6 nt inserted 5′ of HS2. Oligos hs1mutF (5′-GGACCCCTCAGTTGTTCC**GcTT**

caCCTcTTTGGAAAAC) and hs1mutR (5′-GAAATCTT GGTTTTCCAAAgAGG**tgAAgC**GGAACAACT) were used to mutate HS1 (destroys a HaeI site); oligos hs3mutF (5′-CCTTTTTGGAAAACCAAGATgT**CAcgT**TGACG AGCTCAAGCATC) and hs3mutR (5′-GATGCTTGA GCTCGTCA**AcgTG**AcATCTTGGTTTTCCAAAAAGG) were used to mutate HS3 (creates a TaiI site); oligos 6AmutF (5′-CCTTTGACGAGCTAGCTGAAtcAATTC AAAGTTGCCAAGATC) and 6AmutR (5′-GATCTTG GCAACTTTGAATTgaTTCAGCTAGCTCGTCAAAGG) were used to mutate the 6A run (creates a HinfI site); and oligos lys_A746_stop_F (5′-GACGAGCTCAAGC ATCATTTCGTGGACcattaa**TTTG**CTTCGAATTTGG ATACCAGTAATAATGCG) and lys_A746_stop_R (5′-CGCATTATTACTGGTATCCAAATTCGAAG**CAAA** ttaatgGTCCACGAAATGATGCTTGAGCTCGTC) were used to insert 6 nt immediately 5′ of HS2 (creating an in-frame stop codon and an AseI site). Nucleotide changes are indicated in lowercase, bold sequences correspond to the relevant hotspot, and underlined sequences indicate the position of the 6A run. The hs1mutF/hs1mutR oligos were used with pSR812 (*lys2ΔA746,hs1′*) to create pSR815 (*lys2ΔA746,hs1′,hs1mut*); the hs3mutF/hs3mutR oligos were used with pSR786 (*lys2ΔA746*) to create pSR817 (*lys2ΔA746,hs3mut*); the 6AmutF/6AmutR oligos were used with pSR818 (*lys2ΔA746,hs3′,hs3mut*) to create pSR849 (*lys2ΔA746,6Amut,hs3′,hs3mut*); and the lys_A746_stop_F/lys_A746_stop_R oligos were used with pSR582 (*lys2-A767C,T781C*) and pSR786 (*lys2ΔA746*) to create pSR835 (*lys2-5′hs2*) and pSR814 (*lys2ΔA746,5′hs2*), respectively. Relevant mutations were verified by sequencing.

Yeast strain construction

A list of yeast strains used in this study is given in Table 1. All yeast strains are congenic derivatives of SJR195 (*MATα ade2-101$_{oc}$ his3Δ200 ura3ΔNco*) constructed by standard lithium acetate transformation (33). *RAD14* was deleted using a PCR-generated kanMX2 cassette (34) or was disrupted using PvuII-digested pGC2274 (*rad14::hisG-URA3-KAN-hisG*; obtained from G. F. Crouse, Emory University). *REV3* was deleted using a PCR-generated hphMX3 cassette (34) and *RAD30* was deleted using a *rad30Δ::HIS3* fragment from pJM82 (21). Strains containing the *lys2ΔA746* allele or its derivatives were constructed by two-step allele replacement. All *lys2ΔA746*-containing plasmids were targeted to *LYS2* by AflII digestion and transformants were selected on SCD-uracil. Ura$^-$ derivatives that had lost the plasmid were selected on 5-FOA plates and were screened for a Lys$^-$ phenotype. The *lys2-5′hs2* allele was introduced into yeast strains by transformation with AflII-digested pSR835. Following selection for His$^+$ transformants, plasmid pop-outs that retained the *lys2-5′hs2* allele were selected on α-AA medium. The relevant mutations within *LYS2* were confirmed by sequencing.

Mutation rates and spectra

For each strain, two independent isolates and at least 12 cultures per strain were used to determine the mutation rate. Cultures were inoculated in parallel with 5×10^4 cells and then grown nonselectively in 5 ml YEPGE to saturation ($\sim 2 \times 10^8$ cells/ml). Cells were pelleted, washed with 5 ml sterile H_2O and resuspended in 1 ml of sterile H_2O. To assess viable cells and mutants, 100 µl of the appropriate cell dilutions were plated on YEPD and SCD-Lys plates, respectively. All plating was done in duplicate and colonies were counted after three days of growth. Reversion rates and associated 95% confidence intervals were determined by the maximum likelihood method (35,36) and were calculated using the 'Mathematica' program SALVADOR (37). Rates were considered to be different if the 95% confidence intervals did not overlap. The reversion rate of a specific category of frameshift event was determined by multiplying the percentage of the event in the reversion spectrum by the corresponding overall reversion rate.

To obtain mutation spectra, genomic DNA was isolated from purified Lys$^+$ revertants using a glass bead lysis procedure (38). To guarantee independence of each reversion event, only one colony from each culture was used to generate spectra. A portion of the *LYS2* locus containing the reversion window was amplified by PCR

Table 1. Yeast strains

Strain	Relevant genotype	Reference/Source
SJR922	*lys2ΔA746*	Ref. 25
SJR1408	*rad14::hisG-URA3-kan-hisG lys2ΔA746*	Ref. 25
SJR1463	*rad30Δ::HIS3 lys2ΔA746*	OST of SJR922 using pJM82
SJR1479	*rad14::hisG-URA3-kan-hisG rad30Δ::HIS3 lys2ΔA746*	OST of SJR1463 with restriction fragment from pGC2274
SJR1710	*rad14Δ::kan*	OST of SJR195 with PCR fragment
SJR1756	*rad14Δ::kan lys2ΔA746,hs1′-INV*	TST of SJR1710 using pSR813
SJR1779	*rad14Δ::kan lys2ΔA746,hs1′,hs1mut*	TST of SJR1710 using pSR815
SJR1849	*rad14Δ::kan lys2-5′hs2*	TST of SJR1710 using pSR835
SJR1866	*rad14Δ::kan rad30Δ::HIS3*	OST of SJR1710 with PCR fragment from SJR1463
SJR1876	*rad14Δ::kan rad30Δ::HIS3 lys2ΔA746,hs3′,hs3mut*	TST of SJR1866 using pSR818
SJR1878	*rad14Δ::kan lys2ΔA746,hs3′,hs3mut*	TST of SJR1710 using pSR818
SJR2052	*rad14Δ::kan rad30Δ::HIS3 lys2ΔA746,6Amut,hs3′,hs3mut*	TST of SJR1876 using pSR849
SJR2389	*rad14Δ::kan lys2ΔA746,5′hs2*	TST of SJR1710 using pSR814
SJR2640	*rad14Δ::kan revΔ3::hyg lys2-5′hs2*	OST of SJR1849 with PCR fragment

All strains are congenic derivatives of SJR195 (*MATα ade2-101$_{oc}$ his3Δ200 ura3ΔNco*).
OST, one-step allele transplacement; TST, two-step allele transplacement.

and automated DNA sequence analysis of PCR-amplified genomic fragments was performed using the primer MO18 (5′-GTAACCGGTGACGATGAT) at the University of Washington (Seattle) High-Throughput Sequencing Solution Facility. Sequences were analyzed using the Sequence Manager Software (DNA STAR, Inc.). Figures were generated using Adobe Illustrator.

Chi-square analysis was used to determine if a transposed hotspot accumulated a similar proportion of complex events as the original hotspot. The proportion of complex events at the transposed hotspot was considered statistically different from that at the hotspot in its original location if $P < 0.05$.

RESULTS

We have previously shown that, in the absence of NER, Polζ-dependent complex frameshift events accumulate at three distinct hotspots within the *lys2ΔA746* reversion window: HS1, 5′-TTTG**G**; HS2, 5′-TTT**G**; and HS3, 5′-**C**AAA (23,25). At each hotspot, the selected frameshift occurs in a 3A or 3T run, with the predominant base substitution being either a C→A transversion 5′ of the run or a G→T transversion 3′ of the run (indicated in bold in the core hotspot sequences above), respectively. At least for HS1 and HS2, we have shown that the 3′ G is absolutely required for the slippage events in the 3T run (25). This latter observation was the basis for proposing a 'misincorporation-slippage' model in which the base substitution precedes and facilitates the selected slippage event.

There are nine A or T runs ≥3N within the *lys2ΔA746* reversion window, and yet only three of these are hotspots for complex frameshifts. Of the six nonhotspot runs, four have the same core consensus sequence as the hotspots. In order to understand why Polζ-dependent complex frameshifts accumulate at some positions but not others, the current study used two approaches to examine the effect of local sequence context on hotspot activity. First, to determine whether the surrounding sequences are sufficient to confer hotspot activity, we examined whether a hotspot can be functionally transposed to a different position within the reversion window and whether inversion of a hotspot affects its function. Second, we specifically addressed the necessity of sequences adjacent to the 3T run of HS2, but on the opposite side of the site where the associated G→T transversion occurs. Finally, because ∼50% of complex frameshifts have more than one associated base substitution (25), we asked whether the occurrence of multiple base substitutions is uniquely associated with frameshift events at the hotspots, or whether it is a more general property of Polζ-dependent mutagenesis *in vivo*. It should be noted that all experiments reported here were performed in an NER-defective (*rad14Δ*) strain background. In the interest of conciseness, however, the *rad14Δ* allele is not included as part of the relevant genotypes in the sections that follow. Because all strains contain the *rad14Δ* allele, the complex events being examined are assumed to be generated in response to spontaneously occurring lesions that are normally removed by the NER pathway.

Transposition and inversion of HS1

A given sequence could function as a complex hotspot because of its local sequence context, its location on the noncoding versus coding strand, or its specific position within the *lys2ΔA746* reversion window (e.g. because of chromatin-related packaging). To begin to distinguish between these possibilities, we first transposed HS1 to a new location within the reversion window. If only the immediate sequence context is relevant to hotspot activity, then one would predict that the transposed sequence should act as a hotspot for complex frameshifts. Two criteria were used to assess the functionality of the transposed hotspot (HS1′). First, we compared the rate of complex events at HS1′ relative to the original HS1, as well as the proportion of reversion events at HS1 versus HS1′. Second, the pattern of frameshift-associated base substitutions at the new location was compared to that at the original location, as this pattern presumably reflects the underlying mechanism of mutagenesis.

For the transposition of HS1, an 18-bp fragment sharing 13 bp of identity with HS1 was inserted at a unique BglII site located ∼25-bp upstream, thereby creating the *lys2ΔA746,hs1′* allele (Figure 2). In addition to the core TTTGG HS1 sequence, 3-nt upstream of the 3T run and 5-nt downstream of the critical 3′ G were transposed to this position. When Lys^+ revertants of the *lys2ΔA746,hs1′* strain were sequenced, we observed that 50% of the events were 40-bp duplications with endpoints in the 13-bp direct repeats created by the transposition of HS1 (data not shown). This duplication restores the correct reading frame of the *LYS2* gene without introducing stop codons or disrupting function of the encoded protein. To eliminate the direct repeats and hence the duplications from the spectrum, site-directed mutagenesis was used to change the original HS1 sequence to 5′-CG**c**TT**ca**CCT**c**TTT (changes in lowercase bold), creating the *lys2ΔA746,hs1′,hs1mut* allele (Figure 2). The overall reversion rate of the *lys2ΔA746,hs1′,hs1mut* allele was indistinguishable from that of the original *lys2ΔA746* allele (Table 2), and the proportion of complex events at HS1′ (8/193; Supplementary Figure 1) was similar to the proportion at the original HS1 (23/374; $P = 0.42$). Furthermore, at the original HS1, over 95% (22/23) of the complex events had a base substitution at the G residue located 2-nt 3′ of the 3T run, and of these, 50% (11/22) were G→T tranversions (Table 3). At HS1′, seven of the eight complex events were associated with a base substitution at the corresponding 3′ G and six of these base substitutions were G→T transversions (Table 3). The complex frameshift insertion pattern as well as rate at the transposed HS1′ is thus very similar to that at HS1, and we conclude that 13 bp is sufficient to recapitulate the features of HS1 at a new location.

Given that it was possible to functionally move HS1 to a new location, we examined whether the occurrence of complex events at this new site would be affected by inversion of HS1′ (*lys2ΔA746,hs1′-INV* allele; Figure 2).

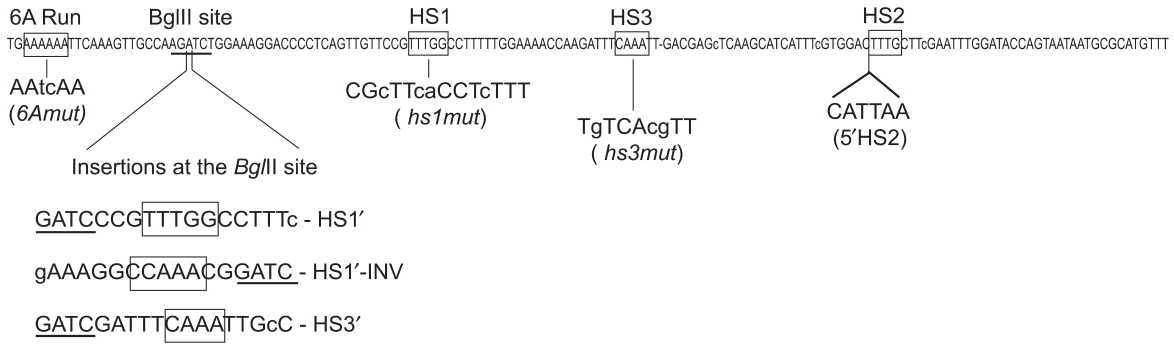

Figure 2. Sequence changes to the *lys2ΔA746* reversion window. The positions of the 6A run (boxed), the unique BglII site where the transposed hotspots sequences were inserted (underlined) and the core HS1-HS3 sequences (boxed) are indicated. The sequences of the insertions or base substitutions used to create specific alleles are indicated below the reversion window sequence. Lowercase letters indicate the site-specific sequence changes.

Table 2. Rates of complex insertions at HS1, HS1′ and HS1′-INV

Relevant genotype	Mutation rate ($\times 10^{10}$)		
	Total Lys$^+$	Complex events at HS1	Complex events at HS1′
lys2ΔA746	58 (47–70)	3.8	NA
lys2ΔA746,hs1′,hs1mut	62 (45–85)	NA	2.2
lys2ΔA746,hs1′-INV	76 (55–98)	4.5	2.3

All strains are *rad14Δ*. Numbers in parentheses following rates are 95% confidence intervals. NA, not applicable.

Inversion not only moves the hotspot sequence from the coding/nontranscribed strand to the noncoding/transcribed strand, but also changes its strandedness during DNA replication. The *LYS2* locus is replicated from an upstream origin (39,40), making the coding strand the template for lagging-strand synthesis. The damaged G that is presumed to initiate misincorporation-slippage at HS1 and HS1′ would thus be located on the lagging-strand template. For HS1′-INV, the corresponding G would be on the leading-strand template.

The overall reversion rate of the *lys2ΔA746,hs1′-INV* allele was not different from that of the *lys2ΔA746* or *lys2ΔA746,hs1′,hs1mut* allele (Table 2). In addition, of the 200 *lys2ΔA746,hs1′-INV* revertants sequenced, six were complex frameshift events at HS1′-INV, which is similar to the proportion of complex events observed at HS1 and HS1′ ($P = 0.20$ and $P = 0.73$, respectively). The coding-strand pattern of complex reversion events at HS1′-INV was the reverse complement of that at HS1 and HS1′. Events at HS1′-INV were thus comprised of addition of an A to the 3A run accompanied by base substitution at a 5′ C, 67% of which were C→A transversions (Table 3). This result is similar to that obtained following inversion of the entire *LYS2* locus, which only reverses the identities of the leading- and lagging-strand templates (23). The data obtained with HS1′-INV indicates that mutagenesis is additionally not affected by the location of the underlying lesion on the transcribed versus nontranscribed strand. Finally, it should be noted that, as at HS1, multiple base substitutions were commonly observed among the complex events at HS1′ and HS1′-INV (3/8 and 3/6, respectively; Table 3).

Table 3. Complex events at HS1, HS1′ and HS1′-INV

Hotspot	Relevant genotype	Coding strand sequence							#
HS1	*lys2ΔA746* ($N = 174$) and *lys2ΔA746,hs1′-INV* ($N = 200$)	C	C	G	TTT	G	***G***	C	
					+		T		5
					+		T	T	2
				T	+		T		2
				T	+		T	T	1
				C	+		T		1
					+		G		2
					+		C		3
				C	+		C		2
					+	A	A	T	1
					+		A		1
				T	+		A		1
					+		A	T	1
				C	+				1
HS1′	*lys2ΔA746,hs1′,hs1mut* ($N = 193$)	C	C	G	TTT	G	***G***	C	
					+		T		3
				T	+		T		2
					+		T	T	1
					+		A		1
					+			T	1
HS1′-INV	*lys2ΔA746,hs1′-INV* ($N = 200$)	G	***C***	C	AAA	C	G	G	
			A		+				2
			A		+	A			1
		A	A		+				1
			G		+				1
			G	G	+				1

All strains are *rad14Δ*. The number of Lys$^+$ revertants sequenced (N) for each hotspot is indicated. The 3′ G that is assumed to represent the site of the initiating lesion is in bold italics.

HS3′ retains some, but not all, of the properties associated with HS3

The complex events at HS3 only predominate in the absence of Polη (Figure 1), suggesting a TLS polymerase hierarchy that is different from that operating at HS1 and HS2 (23). To gain further insight into the nature of HS3, we inserted an 18-bp fragment containing 13 bp of identity to HS3 at the BglII site ~50-bp upstream of HS3 (Figure 2). To prevent duplications from occurring between HS3 and the transposed HS3′, the original HS3 sequence was subjected to site-directed mutagenesis, creating the *lys2ΔA746,hs3′,hs3mut* allele (Figure 2).

Table 4. Rates of complex insertions at HS3 and HS3′

Relevant genotype	Mutation rate ($\times 10^{10}$)		
	Total Lys$^+$	HS3 complex events	HS3′ complex events
lys2ΔA746	58 (47–70)	0.35	NA
rad30Δ lys2ΔA746	53 (39–68)	6.4	NA
lys2ΔA746,hs3′,hs3mut	51 (37–67)	NA	0.34
rad30Δ lys2ΔA746,hs3′,hs3mut	58 (44–72)	NA	4.5
rad30Δ lys2ΔA746,6Amut,hs3′,hs3mut	43 (29–59)	NA	2.6

All strains are *rad14Δ*. Numbers in parentheses following rates are 95% confidence intervals.

Reversion rates and spectra were then examined in both the presence and absence of Polη (*RAD30* and *rad30Δ* backgrounds, respectively).

The Lys$^+$ rates of the *lys2ΔA746,hs3′,hs3mut* and the *rad30Δ lys2ΔA746,hs3′,hs3mut* strains were no different from those of the respective *lys2ΔA746* and *rad30Δ lys2ΔA746* strains (Table 4). Consistent with previous observations with HS3, complex events at HS3′ were prominent only in the absence of Polη; only 1/150 reversion events was a complex event at HS3′ in the *RAD30* strain, while 15/194 events were complex frameshifts at HS3′ in the *rad30Δ* strain (Supplementary Figure 2; $P < 0.01$). In the *rad30Δ* background, the proportion of complex events at HS3′ was similar to ($P = 0.22$) that at HS3 (20/164; Figure 1).

Although the proportions of complex events at HS3 and HS3′ were similar, the patterns of base substitutions were quite different (Table 5). As noted previously, the selected insertion into the 3A run of HS3 is typically accompanied by a base substitution at the 5′ C (18/20 events) and the change most often observed is a C→A transversion (16/18 events). At HS3′, there also was a strong bias for a C→A mutation at the position 5′ of the 3A run (13/15 events). Eight of the 13 mutants containing a C→A mutation, however, also contained a T→A mutation at the adjacent 5′ T residue; no comparable events were seen at HS3. The net result of the tandem changes together with the frameshift at HS3′ was conversion of the 3A run into a run of 6 A's (5′-TTCAAATT to 5′-TAAAAAATT; Table 5).

The run of 6 As created by complex frameshifts at HS3′ is reminiscent of the naturally occurring 6A run located near the 5′ end of the *lys2ΔA746* reversion window, 20-bp upstream of the position of HS3′. We hypothesized that the complex frameshifts at HS3′ might not be the result of the typical Polζ-dependent misincorporation-slippage, but rather might be the result of a templating event involving the 6A run. If this were the case, then mutating the 6A run in the *lys2ΔA746,hs3′,hs3mut* allele should eliminate the templated events. To test this prediction, the 6A run was eliminated by site-directed mutagenesis (Figure 2). In the resulting *lys2ΔA746,6Amut,hs3′,hs3mut* strain, 11 out of 183 complex reversion events were observed at HS3′ (Supplementary Figure 2), which is similar to the proportion of complex events observed at the original HS3 ($P = 0.10$). In terms of the base substitution pattern, only two of the 10 complex events identified at HS3′ in the *lys2ΔA746,6Amut,hs3′,hs3mut* strain had the tandem base substitutions. Even though this reduction (from 8/15 to 2/10) is suggestive of some templating from the 6A run, the shift in the distribution was not significant ($P = 0.10$).

Table 5. Complex events at HS3 and HS3′

Hotspot	Relevant genotype	Coding strand sequence							#
HS3	*rad30Δ lys2ΔA746*	T	T	***C***	AAA	T	T	G	
	($N = 164$)			A	+				13
				A	+		G	A	1
				A	+		A		1
				A	+	A	G		1
			G	T	+				1
			A	T	+				1
					+		G		2
HS3′	*rad30Δ lys2ΔA746,hs3′,hs3mut*	T	T	***C***	AAA	T	T	G	
	($N = 194$)		A	A	+				7
				A	+				2
				A	+		G		1
			A	A	+	T			1
				A	+	A	A		1
				A	+	A			1
					+		G		2
HS3′	*rad30Δ lys2ΔA746,6Amut, hs3′,hs3mut*	T	T	***C***	AAA	T	T	G	
	($N = 183$)			A	+				6
			A	A	+				2
				A	+		G		1
				A	+	A	A		1
				A	+	A			1

All strains are *rad14Δ*. The number of Lys$^+$ revertants sequenced (N) for each hotspot is indicated. The 5′ C that is assumed to represent the site of the initiating lesion is in bold italics.

The sequence 5′ of HS2 is not necessary for the accumulation of complex events

We have previously demonstrated that mutation of the G residue that is 3′ of the selected frameshift at HS1 or HS2 results in the complete loss of the frameshift events (25), but have not previously examined the relevance of specific 5′-flanking sequences. The transpositions of HS1 and HS3 described above suggest that no more than 3-nt upstream of the 3N run where the selected frameshift occurs is important for hotspot activity. To further address the importance of this region, we inserted 6 nt containing a TAA stop codon (5′-CATTAA) immediately 5′ of HS2, creating the *lys2ΔA746,5′hs2* allele (Figure 2). The introduction of a stop codon has the net effect of shortening the *lys2ΔA746* reversion window from 150 bp to 43 bp, which would be expected to eliminate ~90% of the reversion events normally detected. Consistent with this prediction, the overall reversion rate of the *lys2ΔA746,5′hs2* allele was 6-fold less than that of the *lys2ΔA746* allele (Table 6). Furthermore, the proportion of complex frameshifts increased from 12% (20/164) at HS2 for the *lys2ΔA746* allele to 73% (77/106) at HS2′ for the *lys2ΔA746,5′hs2* allele (Supplementary Figure 3). The pattern of complex insertions observed at 5′HS2 was

Table 6. Rates of complex insertions at HS2 and 5′HS2

Relevant genotype	Mutation rate (x 10^{10})		
	Total Lys$^+$	Complex events at HS2	Complex events at 5′HS2
lys2ΔA746	58 (47–70)	3.0	NA
lys2ΔA746,5′hs2	10 (5.9–16)	NA	7.4

All strains are *rad14Δ*. Numbers in parentheses following rates are 95% confidence intervals.

similar to that seen at the original HS2; of the 77 complex frameshifts at 5′HS2, 73 (95%) had a base substitution at the 3′ G, and 69 of these were G→T transversions (Table 7). Finally, 50% (37/77) of the complex events at 5′HS2 had more than one base substitution. The results obtained with the *lys2ΔA746,5′hs2* allele demonstrate that only the sequence 3′ of the 3T run is required to generate complex frameshifts.

Multiple base substitutions are a general property of Polζ-dependent lesion bypass

The misincorporation-slippage model explains the coupling of the predominant base substitution with the selected frameshift at HS1–HS3. It does not, however, account for the occurrence of the multiple base substitutions in 30–50% of the Polζ-dependent complex frameshifts. We have suggested that the multiple mutations likely reflect an extraordinarily low fidelity for Polζ during lesion bypass *in vivo*. Based on the short distance within which the multiple mutations are generated, we estimate that Polζ incorporates <15 nt during a single bypass event, which would be consistent with its known distributive activity *in vitro* (5). To further examine the fidelity of Polζ *in vivo*, we developed a *LYS2*-based reversion assay that can detect the occurrence of multiple base substitutions in the absence of frameshift mutagenesis. In order to focus on an area where Polζ is known to perform lesion bypass in NER-defective strains, we introduced a TAA stop codon adjacent to HS2 in an otherwise wild-type *LYS2* gene. It should be noted that, given the flexible nature of this region of the LYS2 protein, simultaneously changing multiple amino acids should not affect its activity. The stop codon was introduced by inserting 6 nt (5′-CATTAA) immediately 5′ of the 3T run at HS2, creating the *lys2-5′hs2* allele. These are exactly the same nucleotides that were introduced to create the *lys2ΔA746,5′hs2* allele, and so do not affect hotspot activity as assayed in the *lys2ΔA746* system (see above).

The reversion rate of the *lys2-5′hs2* nonsense allele in an NER-defective background was 2.8×10^{-9}, 2-fold lower than that of the *lys2ΔA746* frameshift allele. We sequenced 196 *lys2,5′hs2* revertants and 187 (95%) of these corresponded to 'locus' mutations in which a base substitution inactivated the TAA stop codon (Table 8). The remaining 5% retained the stop codon and presumably had an extragenic suppressor mutation, but were not further characterized. The adjusted rate of mutations that altered the stop codon was 2.6×10^{-9}, and all possible

Table 7. Complex events at HS2 and 5′HS2

Hotspot	Relevant strain genotype	Coding strand sequence											#
		G	T	G	G	A	C	TTT	***G***	C	T		
HS2	*lys2ΔA746 and rad30Δ lys2ΔA746* ($N = 338$)							+	T				10
							T	+	T				3
								+	T	T			1
						T	T	+	T				2
								+	A	A			2
								+	A				2
								+	C				4
		C	A	T	T	A	A	TTT	***G***	C	T		
5′HS2	*lys2ΔA746,5′hs2* ($N = 106$)							+	T				29
						T		+	T				18
						T	T	+	T				13
							T	+	T	T			2
						T	T	+	T	T			2
			T			T	T	+	T	T			2
								+	T			C	2
								+	T	T			1
								+	A				3
								+	C				1
								+		T			1
							T	+					1
								+		G			1
						T		+					1

All strains are *rad14Δ*. The number of Lys$^+$ revertants sequenced (N) for each hotspot is indicated. The 3′ G that is assumed to represent the site of the initiating lesion is in bold italics.

Table 8. Base substitutions associated with *lys2-5′hs2*

Relevant strain genotype	Coding strand sequence											#
	C	A	T	**T**	**A**	**A**	TTT	***G***	C	T		
lys2-5′hs2 ($N = 187$)				C								30
				G								14
				A								10
					T							26
					C							25
						T						40
						C						22
					C	T						1
					T	T						1
				C		T						1
	T	T			T	T		T				1
		T			T	T		T				6
					T	T		T				4
						T		T				2
		T				T		T				1
					T	A		T				1
					T	T		A				1
					T			T				1
rev3Δ lys2-5′hs2 ($N = 92$)				C								46
				G								4
				A								3
					T							1
					C							10
						T						17
						C						9
				C	C							1
					T	T						1

All strains are *rad14Δ*. The number of Lys$^+$ revertants sequenced (N) for each hotspot is indicated. The TAA stop codon is in bold and underlined; the 3′ G that is assumed to represent the site of the initiating lesion is in bold italics.

base substitutions were observed at each position within the stop codon (e.g. the 5′ T was mutated to A, C or G). In 11% of the revertants (20/187), there was an additional base substitution that accompanied the selected mutation. Not only did the majority (17/20) of these multiple events have a mutation at the 3′ G implicated in complex frameshifts at HS2, but 95% (16/17) of the base substitutions at this position were G → T transversions. Because of this striking pattern, we speculate that the same lesion probably initiates both complex frameshifts at HS2 and multiple base substitutions at 5′HS2. Finally, of the 17 nonsense mutations accompanied by a change at the 3′ G, 14 had additional base substitutions, a pattern that mirrors that seen with the complex frameshifts.

The dependence of nonsense reversion events in the *lys2,5′hs2* assay on the activity of Polζ was examined by deleting *REV3*. The overall Lys^+ rate in the *rev3* mutant was 1.3×10^{-9}, and of 157 revertants sequenced 59% (92/157) were locus revertants. Adjusting the total reversion rate to reflect this proportion yielded a nonsense reversion rate of 7.5×10^{-10}. Polζ is thus required for ~70% of the locus mutations in the *lys2,5′hs2* assay. Although all possible mutations were observed at each position of the stop codon, the proportions of specific mutation types were very different in the *REV3* versus *rev3* background. For example, A → T transversions at the second position of the stop codon comprised 14% (26/187) of the reversion events in the *REV3* strain, but only 2% (2/92) of the events in the *rev3* mutant. Of the 92 locus revertants analyzed from the *rev3* mutant, only two contained more than a single base substitution and neither of these involved the 3′ G. The nonsense reversion data thus indicate that Polζ generates the majority of the damage-initiated multiple changes in the *lys2,5′hs2* assay. It should be noted that neither the frameshift reversion nor the base substitution assay directly selects for mutations at the 3′ G, which precludes a precise determination of how frequently Polζ introduces collateral mutations during a single lesion bypass event. Even so, the results obtained with these assays underscore the low fidelity of this polymerase and document its ability to introduce multiple mutations within a short stretch of DNA *in vivo*.

DISCUSSION

The accumulation of Polζ-dependent complex frameshifts at three distinct hotspots (HS1–HS3) within the *lys2ΔA746* reversion window of NER-defective strains provides a unique mutational signature for TLS by this polymerase. The strikingly similar base substitution pattern at each hotspot (G•C → T•A transversion) suggests a common mechanism of mutagenesis in which bypass of damage at a G•C base pair facilitates subsequent slippage within a 3N run to generate the selected frameshift. In support of this 'misincorporation-slippage' mechanism, we have previously demonstrated that the key G•C base pair is required for slippage within the 3N run of HS1 and HS2. Because the model predicts that the relevant lesion is encountered 'before' the 3N run during DNA synthesis, the initiating damage would be to the guanine of the G•C base pair. While a correctly positioned guanine appears to be necessary for the Polζ-dependent complex frameshifts, it is not sufficient, as there are additional core hotspot sequences (a C preceding or a G following a 3N run on the coding strand) that do not accumulate these events.

The ability of a core sequence element to function as a hotspot for complex frameshifts could be due to local sequence context beyond the critical GC base pair, location on the coding versus noncoding strand of *LYS2*, or position within local chromatin structure. Any of these could influence the accumulation of the initiating lesion, the repair of the lesion by the remaining base excision repair pathway, and/or its bypass by a competing, Polζ-independent mechanism. In the current study, we addressed the issue of immediate sequence context versus absolute position of the core hotspot element by transposing 13 bp of identity to HS1 or HS3 to a new location within the reversion window, yielding HS1′ and HS3′, respectively. In addition, we examined the effect of HS1 position on the coding versus noncoding strand of *LYS2* by inverting the transposed sequence to generate HS1′-INV. Figure 3 summarizes these as well as additional hotspot manipulations.

In considering the functionality of a transposed or inverted hotspot, we examined both the rate of complex events as well as the spectrum of associated base substitutions relative to the original hotspot. In the case of both HS1′ and HS1′-INV, there appeared to be a complete recapitulation of the relevant features of HS1. Thirteen base pairs was thus sufficient for complete activity of HS1, and thus neither the precise location nor the orientation of HS1 within the reversion window was critical for the accumulation of the initiating lesion or for Polζ-dependent bypass. Although 13 bp was sufficient for HS1 activity, our analyses do not address the minimal sequence requirement. The observation that the precise sequence upstream of HS2 is irrelevant (see below), however, suggests that only sequences on the same side of the 3N run as the presumptive initiating lesion are important. That some sequence in addition to the core HS1 sequence (5′-TTTGG) must be necessary is suggested by the occurrence of this precise sequence at two locations within the reversion window that do not accumulate complex frameshifts. Regardless of the exact extent of sequence homology required, it is striking that a relatively discrete segment of DNA surrounding HS1 can be moved and inverted and still maintain its mutagenic properties. Finally, the activity of the inverted segment indicates that, at least in the case of HS1, neither the location of the critical guanine on leading- versus lagging-strand template nor on the transcribed versus nontranscribed strand of *LYS2* is important.

Whereas the results obtained with the transposition and inversion of HS1 were straightforward, those obtained with HS3′ were not as clear. As with HS3, complex events accumulated at HS3′ only in the absence of Polη. The patterns of the complex frameshift events at HS3′ were different from those at HS3, however, with the majority of reversion events at HS3′ having the net effect of creating a 6A run rather than the 5A run typical of the HS3 complex events (Table 3). One possible explanation for the creation of the novel 6A run at HS3′ is templating involving the

naturally occurring 6A run near the 5′ end of the reversion window (41). The closer proximity of the transposed HS3′ to this run might facilitate the realignment required for such templating. Elimination of the upstream 6A run reduced, but did not eliminate, the proportion of complex frameshifts that created a 6A run at HS3′. Although this reduction is consistent with some templating occurring, there may be additional mechanisms operating at the transposed HS3′.

In addition to examining the abilities of hotspots to be transposed and inverted, we also examined the effect of altering the sequence immediately 5′ of the 3T run at HS2. The misincorporation-slippage model predicts that slippage in the 3T run is precipitated by a prior event (i.e. synthesis past a damaged guanine), making the specific sequence of the region 3′ of the run critical. As we showed previously, the presence of the 3′ G is indeed required to generate slippage events in the 3T run that revert the *lys2ΔA746* allele (25). In contrast, the model predicts that the sequence of the region immediately 5′ of the 3T run should be relatively unimportant. To test this prediction, six heterologous base pairs, three of which specified an ochre stop codon, were inserted immediately 5′ of the 3T run (5′HS2; see Figure 3). The rate of complex events at 5′-HS2 was similar to that at HS2, a result that supports a misincorporation-slippage mechanism for generating complex frameshifts.

The misincorporation-slippage model accounts for the co-occurrence of the primary base substitution and the selected frameshift in the *lys2ΔA746* assay, but it does not readily explain the additional base substitutions present in 30–50% of the Polζ-dependent complex frameshifts. These additional mutations occur within 3 bp of the 3N run where the selected frameshift occurs and are assumed to arise during a single round of TLS. They thus appear to be distinct from the mutation 'showers' that can spread over hundreds of base-pairs in other systems (42). We have suggested that the multiple base substitutions in our assay reflect the extremely low fidelity of Polζ on undamaged DNA, and there is no obvious reason why this should be uniquely associated with frameshift mutagenesis. The fact that we were able to insert 6-bp upstream of HS2 without affecting the accumulation of complex frameshifts at this site afforded the opportunity to examine whether base substitutions selected adjacent to HS2 might also be accompanied by additional base substitutions. We thus inserted the same 6 bp (5′-CAATAA) into an otherwise wild-type *LYS2* allele instead of into the *lys2ΔA746* allele. This introduced an in-frame TAA stop codon, reversion of which was selected on lysine-deficient

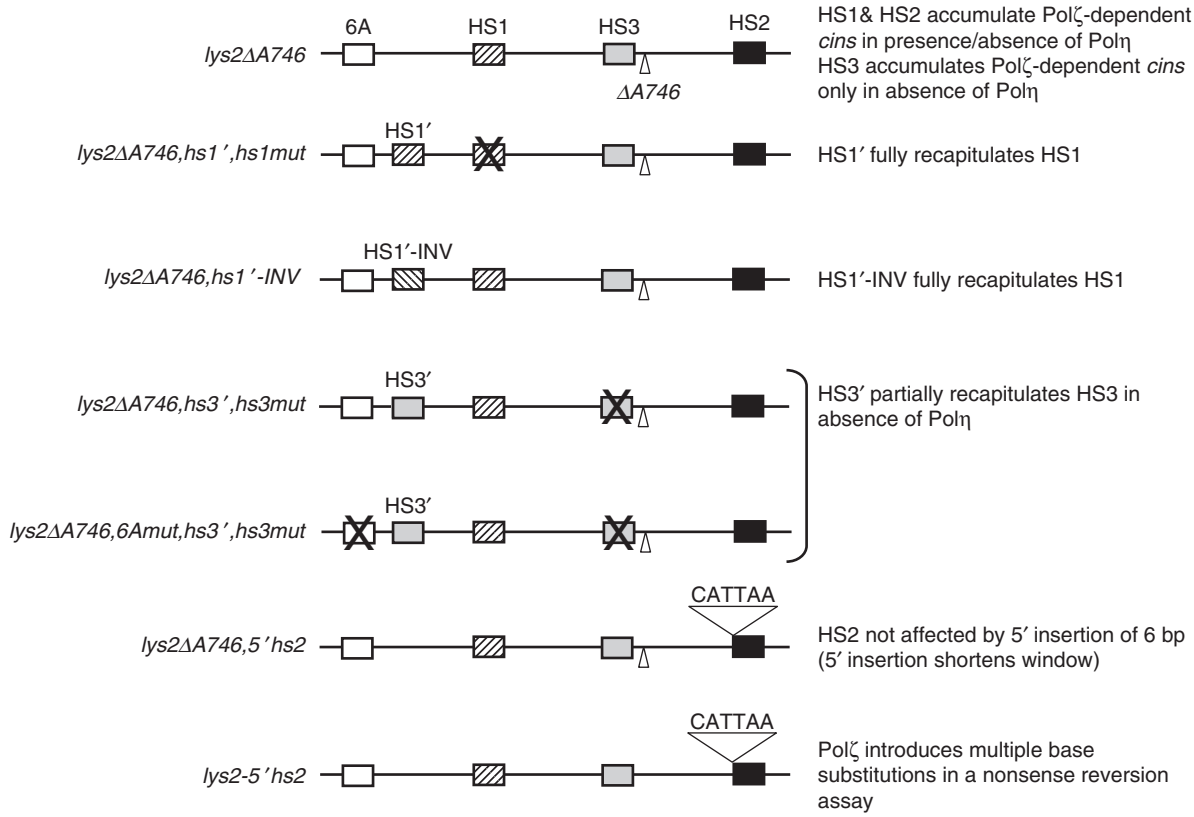

Figure 3. Summary of sequence alterations to the *lys2ΔA746* reversion window. The relative positions of key elements (HS1–HS3, transposed hotspots, the mutated 6A run, the ΔA746 mutation) within the 150-bp reversion window are indicated. An 'X' through an element indicates its elimination by site-directed mutagenesis. The allele names that correspond to the sequence changes are indicated to the left of each cartoon and the relevant results are summarized to the right.

medium. Among the selected nonsense revertants, ~10% contained multiple ('complex') base substitutions. Although this proportion is somewhat lower than that observed among the complex frameshifts, it is very similar to that reported recently by Zhong *et al*. (26). In their analysis, the mutagenic activity of purified Polζ on an undamaged *lacZ* template was examined using a gap-filling assay. Among the forward mutations introduced by Polζ, 4–30% were accompanied by additional, closely spaced mutations.

Of the complex base substitutions identified in the nonsense reversion assay, most (17/20) had a G→T transversion at precisely the same position as seen in the complex frameshifts at HS2. This striking similarity suggests that a single lesion probably initiates both types of complex event. As was the case with the complex frameshifts, the complex base substitutions were confined to a narrow window surrounding the selected base substitution and were strongly dependent on the presence of Polζ. Whether Polζ is recruited to bypass the underlying lesion or simply to extend from a lesion-base mispair created by another DNA polymerase cannot be ascertained in this system, although the additional base-base mismatches are likely to be directly introduced (and extended) by Polζ. An interesting issue concerns the possible removal of Polζ-dependent errors by either the proofreading activity of a replicative DNA polymerase or by the mismatch repair machinery. Such potential editing may be relevant to the mechanism of lesion bypass. If lesion bypass in this system corresponds to a gap-filling reaction behind the replication fork as opposed to a polymerase switch at the fork, then there may well be no editing of the mistakes introduced by Polζ. Experiments are currently in progress that will address whether or not the extraneous base substitutions seen among the complex frameshifts in the *lys2ΔA746* assay are subject to subsequent mismatch repair.

In summary, the experiments reported here reveal several novel features of the Polζ-dependent mutagenesis initiated by persistent spontaneous lesions in NER-defective yeast. First, the sequences identified previously as hotspots for complex frameshifts within the *lys2ΔA746* reversion window can be transposed and inverted, suggesting that both lesion accumulation and bypass are determined solely by local sequence context in this system. Second, the observation that a specific sequence is required on only one side of the run where the selected frameshift occurs further supports a misincorporation-slippage mechanism for this type of mutagenesis. Finally, the results obtained using a nonsense reversion assay indicate that the introduction of multiple mutations within a short stretch of DNA is a general property of Polζ-associated lesion bypass *in vivo*. Under conditions of general stress or when high levels of localized mutagenesis are advantageous, selective recruitment of Polζ, or similarly error-prone polymerases, would thus be expected to accelerate evolutionary processes.

SUPPLEMENTARY DATA

Supplementary Data are available at NAR Online.

ACKNOWLEDGEMENTS

We thank Shannon Hatcher for helping with the sequencing experiments and members of the lab for their discussions throughout the course of this work. We are especially grateful to Jan Drake for his insightful comments on the article. This work was supported by National Institutes of Health (RO1 GM064769 to S.J-R., T32 GM08367 to A.L.A.); Emory University Graduate Division of Biological and Biomedical Sciences (A.L.A. and B.K.M.). Funding to pay the Open Access publication charges for this article was provided by NIH (RO1 GM064769).

Conflict of interest statement. None declared.

REFERENCES

1. Kool,E.T. (2002) Active site tightness and substrate fit in DNA replication. *Annu. Rev. Biochem.*, **71**, 191–219.
2. Baynton,K. and Fuchs,R.P. (2000) Lesions in DNA: hurdles for polymerases. *Trends Biochem. Sci.*, **25**, 74–79.
3. Prakash,S., Johnson,R.E. and Prakash,L. (2005) Eukaryotic translesion synthesis DNA polymerases: specificity of structure and function. *Annu. Rev. Biochem.*, **74**, 317–353.
4. Kunkel,T.A. (2004) DNA replication fidelity. *J. Biol. Chem.*, **279**, 16895–16898.
5. Nelson,J.R., Lawrence,C.W. and Hinkle,D.C. (1996) Thymine-thymine dimer bypass by yeast DNA polymerase ζ. *Science*, **272**, 1646–1649.
6. Johnson,R.E., Yu,S.L., Prakash,S. and Prakash,L. (2003) Yeast DNA polymerase ζ is essential for error-free replication past thymine glycol. *Genes Dev.*, **17**, 77–87.
7. Johnson,R.E., Washington,M.T., Haracska,L., Prakash,S. and Prakash,L. (2000) Eukaryotic polymerases ι and ζ act sequentially to bypass DNA lesions. *Nature*, **406**, 1015–1019.
8. Quah,S.-K., Von Borstel,R.C. and Hastings,P.J. (1980) The origin of spontaneous mutation in *Saccharomyces cerevisiae*. *Genetics*, **96**, 819–839.
9. Lawrence,C.W. (2002) Cellular roles of DNA polymerase ζ and Rev1 protein. *DNA Repair*, **1**, 425–435.
10. Nelson,J.R., Lawrence,C.W. and Hinkle,D.C. (1996) Deoxycytidyl transferase activity of yeast REV1 protein. *Nature*, **382**, 729–731.
11. Nelson,J.R., Gibbs,P.E.M., Nowicka,A.M., Hinkle,D.C. and Lawrence,C.W. (2000) Evidence for a second function for *Saccharomyces cerevisiae* Rev1p. *Mol. Microbiol.*, **37**, 549–554.
12. Washington,M.T., Minko,I.G., Johnson,R.E., Haracska,L., Harris,T.M., Lloyd,R.S., Prakash,S. and Prakash,L. (2004) Efficient and error-free replication past a minor-groove N2-guanine adduct by the sequential action of yeast Rev1 and DNA polymerase ζ. *Mol. Cell Biol.*, **24**, 6900–6906.
13. Acharya,N., Haracska,L., Johnson,R.E., Unk,I., Prakash,S. and Prakash,L. (2005) Complex formation of yeast Rev1 and Rev7 proteins: a novel role for the polymerase-associated domain. *Mol. Cell Biol.*, **25**, 9734–9740.
14. D'Souza,S. and Walker,G.C. (2006) Novel role for the C terminus of *Saccharomyces cerevisiae* Rev1 in mediating protein-protein interactions. *Mol. Cell Biol.*, **26**, 8173–8182.
15. Guo,C., Fischhaber,P.L., Luk-Paszyc,M.J., Masuda,Y., Zhou,J., Kamiya,K., Kisker,C. and Friedberg,E.C. (2003) Mouse Rev1 protein interacts with multiple DNA polymerases involved in translesion DNA synthesis. *EMBO J.*, **22**, 6621–6630.
16. Haracska,L., Unk,I., Johnson,R.E., Johansson,E., Burgers,P.M., Prakash,S. and Prakash,L. (2001) Roles of yeast DNA polymerases δ and ζ and of Rev1 in the bypass of abasic sites. *Genes Dev.*, **15**, 945–954.
17. Johnson,R.E., Prakash,S. and Prakash,L. (1999) Efficient bypass of a thymine-thymine dimer by yeast DNA polymerase, Polη. *Nature*, **283**, 1001–1004.
18. Haracska,L., Yu,S.L., Johnson,R.E., Prakash,L. and Prakash,S. (2000) Efficient and accurate replication in the presence of

7,8-dihydro-8-oxoguanine by DNA polymerase η. *Nat. Genet.*, **25**, 458–461.
19. Zhang,Y., Yuan,F., Wu,X., Rechkoblit,O., Taylor,J.S., Geacintov,N.E. and Wang,Z. (2000) Error-prone lesion bypass by human DNA polymerase η. *Nucleic Acids Res.*, **28**, 4717–4724.
20. Roush,A.A., Suarez,M., Friedberg,E.C., Radman,M. and Siede,W. (1998) Deletion of the *Saccharomyces cerevisiae gene RAD30* encoding an *Escherichia coli* DinB homolog confers UV radiation sensitivity and altered mutability. *Mol. Gen. Genet.*, **257**, 686–692.
21. McDonald,J.P., Levine,A.S. and Woodgate,R. (1997) The *Saccharomyces cerevisiae RAD30* gene, a homologue of *Escherichia coli dinB* and *umuC*, is DNA damage inducible and functions in a novel error-free postreplication repair mechanism. *Genetics*, **147**, 1557–1568.
22. Minesinger,B.K., Abdulovic,A.L., Ou,T.M. and Jinks-Robertson,S. (2006) The effect of oxidative metabolism on spontaneous Pol ζ-dependent translesion synthesis in *Saccharomyces cerevisiae*. *DNA Repair*, **5**, 226–234.
23. Abdulovic,A.L., Minesinger,B.K. and Jinks-Robertson,S. (2007) Identification of a strand-related bias in the PCNA-mediated bypass of spontaneous lesions by yeast Polη. *DNA Repair*, **6**, 1307–1318.
24. Minesinger,B.K. and Jinks-Robertson,S. (2005) Roles of RAD6 epistasis group members in spontaneous Polζ-dependent translesion synthesis in *Saccharomyces cerevisiae*. *Genetics*, **169**, 1939–1955.
25. Harfe,B.D. and Jinks-Robertson,S. (2000) DNA polymerase ζ introduces multiple mutations when bypassing spontaneous DNA damage in *Saccharomyces cerevisiae*. *Mol. Cell*, **6**, 1491–1499.
26. Zhong,X., Garg,P., Stith,C.M., Nick McElhinny,S.A., Kissling,G.E., Burgers,P.M. and Kunkel,T.A. (2006) The fidelity of DNA synthesis by yeast DNA polymerase ζ alone and with accessory proteins. *Nucleic Acids Res.*, **34**, 4731–4742.
27. Sherman,F. (1991) Getting started with yeast. *Methods Enzymol.*, **194**, 3–20.
28. Boeke,J.D., Trueheart,J., Natsoulis,G. and Fink,G.R. (1987) 5-fluoroorotic acid as a selective agent in yeast molecular genetics. *Methods Enzymol.*, **154**, 164–175.
29. Chattoo,F.F., Sherman,F., Azubalis,D.A., Fjellstedt,T.A., Mehnert,D. and Ogur,M. (1979) Selection of *lys2* mutants of the yeast *Saccharomyces cerevisiae* by the utilization of α-aminoadipate. *Genetics*, **93**, 51–65.
30. Harfe,B.D. and Jinks-Robertson,S. (1999) Removal of frameshift intermediates by mismatch repair proteins in *Saccharomyces cerevisiae*. *Mol. Cell Biol.*, **19**, 4766–4773.
31. Sikorski,R.S. and Hieter,P. (1989) A system of shuttle vectors and yeast host strains designed for efficient manipulation of DNA in *Saccharomyces cerevisiae*. *Genetics*, **122**, 19–27.
32. Fleig,U.N., Pridmore,R.D. and Philippsen,P. (1986) Construction of *LYS2* cartridges for use in genetic manipulations of *Saccharomyces cerevisiae*. *Gene*, **46**, 237–245.
33. Gietz,R.D. and Woods,R.A. (2002) Transformation of yeast by lithium acetate/single-stranded carrier DNA/polyethylene glycol method. *Methods Enzymol.*, **350**, 87–96.
34. Wach,A., Brachat,A., Pohlmann,R. and Philippsen,P. (1994) New heterologous modules for classical or PCR-based gene disruptions in *Saccharomyces cerevisiae*. *Yeast*, **10**, 1793–1808.
35. Sarkar,S., Ma,W.T. and Sandri,G.H. (1992) On fluctuation analysis: a new, simple and efficient method for computing the expected number of mutants. *Genetica*, **85**, 173–179.
36. Rosche,W.A. and Foster,P.L. (2000) Determining mutation rates in bacterial populations. *Methods*, **20**, 4–17.
37. Zheng,Q. (2002) Statistical and algorithmic methods for fluctuation analysis with SALVADOR as an implementation. *Math. Biosci.*, **176**, 237–252.
38. Hoffman,C.S. and Winston,F. (1987) A ten-minute DNA preparation from yeast efficiently releases autonomous plasmids for transformation of *Escherichia coli*. *Gene*, **57**, 267–272.
39. Tran,H.T., Degtyareva,N.P., Koloteva,N.N., Sugino,A., Masumoto,H., Gordenin,D.A. and Resnick,M.A. (1995) Replication slippage between distant short repeats in *Saccharomyces cerevisiae* depends on the direction of replication and the *RAD50* and *RAD52* genes. *Mol. Cell Biol.*, **15**, 5607–5617.
40. Freudenreich,C.H., Stavenhagen,J.B. and Zakian,V.A. (1997) Stability of a CTG/CAG trinucleotide repeat in yeast is dependent on its orientation in the genome. *Mol. Cell Biol.*, **17**, 2090–2098.
41. Ripley,L.S. (1990) Frameshift mutation: determinants of specificity. *Annu. Rev. Genet.*, **24**, 189–213.
42. Drake,J.W. (2007) Mutations in clusters and showers. *Proc. Natl Acad. Sci. USA*, **104**, 8203–8204.